

Total Synthesis and Antibacterial Activity of Dysidavarone A

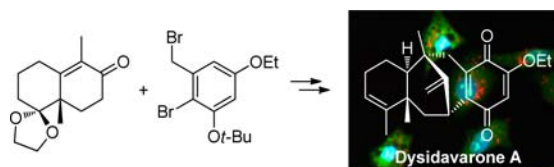
Björn Schmalzbauer,[†] Jennifer Herrmann,[‡] Rolf Müller,^{*,‡} and Dirk Menche^{*,†}

Kekulé-Institut für Organische Chemie und Biochemie, University of Bonn, Gerhard-Domagk-Str. 1, 53121 Bonn, Germany, and Helmholtz-Institut für Pharmazeutische Forschung Saarland (HIPS) and Institut für Pharmazeutische Biotechnologie, Universität des Saarlandes, Gebäude C 2.3, 66123 Saarbrücken, Germany

rom@mx.uni-saarland.de; dirk.menche@uni-bonn.de

Received January 18, 2013

ABSTRACT



A concise total synthesis of dysidavarone A possessing the new “dysidavarane” carbon skeleton has been accomplished by a convergent strategy, involving a stereoselective reductive alkylation of a Wieland-Miescher type ketone under Birch conditions and an advantageous intramolecular palladium-catalyzed α -arylation of a sterically hindered ketone. Dysidavarone A showed potent antimicrobial and antiproliferative activities based on characteristic morphological changes of treated cells.

The dysidavarones A–D present structurally unique marine natural products that were recently isolated from the sponge *Dysidea avara*.¹ As shown in Scheme 1 for dysidavarone A **1**, the 3D architectures of these quinone sesquiterpenes are characterized by an unprecedented, challenging tetracyclic core that is presumably derived from a rearranged drimane skeleton.¹ Preliminary biological evaluations have demonstrated that they possess antiproliferative activities against various human cancer cell lines as well as inhibitory activities against protein tyrosine phosphatase 1B (PTP1B).¹ The postulated tricyclic biosynthetic precursors, avaron and avarol, show a wide spectrum of biological activity and low toxicity,² ranging

from antibacterial,³ cytostatic,⁴ anti-inflammatory,⁵ antiplatelet,⁶ antioxidant,⁷ and anti-HIV⁸ activity. Moreover, avarol is a potent inhibitor of the cytokine TNF- α , making it attractive for the treatment of inflammatory diseases such as psoriasis.⁹ A more detailed biological evaluation of the dysidavarones themselves, however, has been hampered by the scarcity of these natural products. The intriguing new skeleton together with the sparse natural supply attracted our interest in developing a total synthesis of this unique class of natural products, not only for unambiguous structural assignment, but also to support further biological evaluations. Herein, we report the first total synthesis of dysidavarone A by a highly concise strategy involving an advantageous intramolecular α -arylation of an elaborate ketone. Notably, this presents the first

[†] University of Bonn.

[‡] Universität des Saarlandes.

(1) Jiao, W. H.; Huang, X. J.; Yang, J. S.; Yang, F.; Piao, S. J.; Gao, H.; Li, J.; Ye, W. C.; Yao, X. S.; Chen, W. S.; Lin, H. W. *Org. Lett.* **2012**, *14*, 202.

(2) Atta-ur-Rahman *Studies in Natural Products Chemistry*; Elsevier: Oxford, UK, 2012; Vol. 36, pp 189–218.

(3) Seibert, G.; Raether, W.; Dogović, N.; Gasić, M. J.; Zahn, R. K.; Müller, W. E. *Zbl. Bakt. Hyg.* **1985**, *260A*, 379–386.

(4) (a) Müller, W. E.; Maidhof, A.; Zahn, R. K.; Schröder, H. C.; Gasić, M. J.; Heidemann, D.; Bernd, A.; Kurulec, B.; Eich, E.; Seibert, G. *Cancer Res.* **1985**, *45*, 4822–4826. (b) De Giulio, A.; De Rosa, S.; Stazzullo, G.; Diliberto, L.; Obino, P.; Marongiu, M. E.; Pani, A.; La Colla, P. *Antivir. Chem. Chemother.* **1991**, *2*, 223–227.

(5) Ferrándiz, M. L.; Sanz, M. J.; Bustos, G.; Payá, M.; Alcaraz, M. J.; De Rosa, S. *Eur. J. Pharmacol.* **1994**, *253*, 75–82.

(6) Belisario, M. A.; Maturó, M.; Avagnale, G.; De Rosa, S.; Scopacasa, F.; De Caterina, M. *Pharmacol. Toxicol.* **1996**, *79*, 300–304.

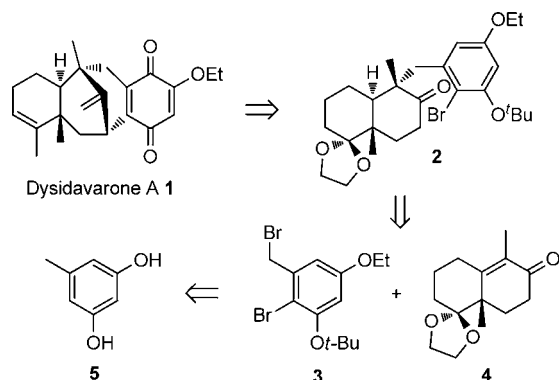
(7) (a) Pejín, B.; Iodice, C.; Tommonaro, G.; De Rosa, S. *J. Nat. Prod.* **2008**, *71*, 1850–1853. (b) Belisario, M. A.; Maturó, M.; Pecce, R.; De Rosa, S.; Villani, G. R. *Toxicology* **1992**, *72*, 221–233.

(8) (a) Sarin, P. S.; Sun, D.; Thornton, A.; Müller, W. E. G. *J. Natl. Cancer Inst.* **1987**, *78*, 663–666. (b) Loya, S.; Hizi, A. *FEBS Lett.* **1990**, *269*, 131–134.

(9) Amigó, M.; Payá, M.; Braza-Boils, A.; De Rosa, S.; Terencio, M. C. *Life Sci.* **2008**, *82*, 256–264.

total synthesis of a dysidavarone-type natural product and unequivocally confirms the full 3D architecture of this class of compounds. Furthermore, the convergent sequence was readily scalable and enabled more detailed biological evaluation of dysidavarone A revealing potent antibacterial and antiproliferative activities as well as specific morphological changes of treated cells.

Scheme 1. Retrosynthesis Analysis of Dysidavarone A

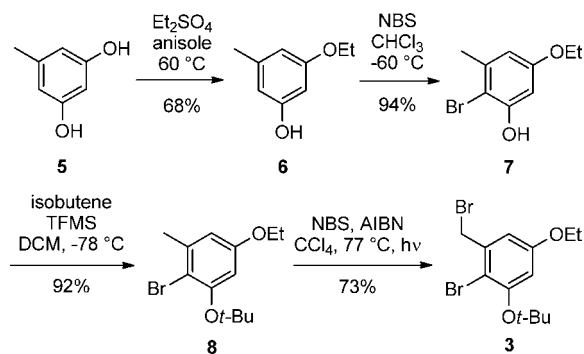


As shown in Scheme 1, our retrosynthetic plan relied on protected phenol **2** as a late-stage intermediate, which was planned to be converted to the tetracyclic core of **1** by a challenging intramolecular palladium-catalyzed α -arylation.¹⁰ The quinone functionality in turn was expected to arise at a late step of the route after liberation of the labile phenol by oxidation. Intermediate **2** in turn should be generated through a stereoselective reductive alkylation under Birch type conditions from known Wieland-Miescher type ketone **4**¹¹ with orcinol **5** derived benzyl bromide **3**.

As shown in Scheme 2, the synthesis of aromatic building block **3** started from orcinol **5**, which was monoethylated with diethylsulfate¹² followed by selective bromination of the aromatic core with NBS.¹³ After protection of the remaining phenol as a *tert*-butyl ether,¹⁴ the benzylic position was brominated with NBS/AIBN.

The 1,2-dioxolane protected Wieland-Miescher type ketone **4** was prepared in three steps in enantiopure form according to a previously reported procedure involving an organo-catalyzed Hajos-Parish-Eder-Sauer-Wiechert type aldol condensation.¹¹ The *ee* of the crude product of the condensation as determined by chiral HPLC analysis was very good (95%) despite the use of (*L*)- α -Phenylalanine in contrast to (*L*)- β -Phenylalanine, which was used in the

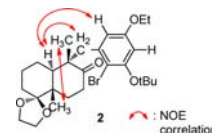
Scheme 2. Synthesis of Benzyl Bromide **3**



original work. Recrystallization from *n*-pentane raised the *ee* to excellent 99.9%. As shown in Scheme 3, the stereoselective coupling of the two building blocks **3** and **4** by a reductive alkylation under Birch conditions proceeded with good yields (72%) and furnished the desired diastereomer **2** with high selectivities (*dr* > 20:1).^{15,16}

The results of the pivotal intramolecular α -arylation of ketone **2** are summarized in Table 1. No conversion was observed in initial studies with catalytic amounts of $\text{PdCl}_2(\text{PPh}_3)_2$ ¹⁷ and $(\text{DtBPF})\text{PdCl}_2$,¹⁸ while $\text{Pd}(\text{OAc})_2$ in the absence of ligands only led to degradation.¹⁹ Also, a combination of $\text{Pd}(\text{OAc})_2$ with $\text{P}(t\text{-Bu})_3$ ²⁰ was tried but again no conversion was observed. It was assumed that the sterical hindrance of the two bulky residues in the *ortho* position of the bromine might prevent the reaction. Therefore, we attempted to cleave the *tert*-butyl ether to evaluate the unprotected phenol. However, these attempts likewise failed due to the high instability of the liberated phenol. Finally, a combination of $\text{Pd}(\text{OAc})_2$ with ligand **9**, which was developed by the group of Buchwald, led to a successful ring-closure in good yields (66%) considering the complexity and high steric hindrance of the substrate.¹⁹ Catalyst-loadings of 10 mol % were required to achieve complete conversion. Use of XPhos-precatalyst²¹ also resulted in product formation, but in lower yields and

(15) The stereochemistry of **2** was confirmed by NMR methods:



(16) This type of reductive alkylation often served as key-step in the total synthesis of sesquiterpenoid quinones and hydroquinones albeit with simpler aromates. For some examples, see: (a) Sarma, A. S.; Chattopadhyay, P. *J. Org. Chem.* **1982**, *47*, 1727–1731. (b) An, J.; Wiemer, D. F. *J. Org. Chem.* **1996**, *61*, 8775–8779. (c) Stahl, P.; Kissau, L.; Mazitschek, R.; Huwe, A.; Furet, P.; Giannis, A.; Waldmann, H. *J. Am. Chem. Soc.* **2001**, *123*, 11586–11593. (d) Sakurai, J.; Oguchi, T.; Watanabe, K.; Abe, H.; Kanno, S.; Ishikawa, M.; Katoh, T. *Chem.—Eur. J.* **2008**, *14*, 829–837.

(17) Muratake, H.; Natsume, M. *Tetrahedron Lett.* **1997**, *38*, 7581–7582.

(18) Grasa, G. A.; Colacot, T. *J. Org. Lett.* **2007**, *9*, 5489–5492.

(19) Fox, J. M.; Huang, X.; Chieffi, A.; Buchwald, S. L. *J. Am. Chem. Soc.* **2000**, *122*, 1360–1370.

(20) Kawatsura, M.; Hartwig, J. F. *J. Am. Chem. Soc.* **1999**, *121*, 1473–1478.

(10) For a review on metal-catalyzed α -arylation of carbonyl see: (a) Johansson, C. C. C.; Colacot, T. *J. Angew. Chem., Int. Ed.* **2010**, *49*, 676–707. (b) Bellina, F.; Rossi, R. *Chem. Rev.* **2010**, *110*, 1082–1146.

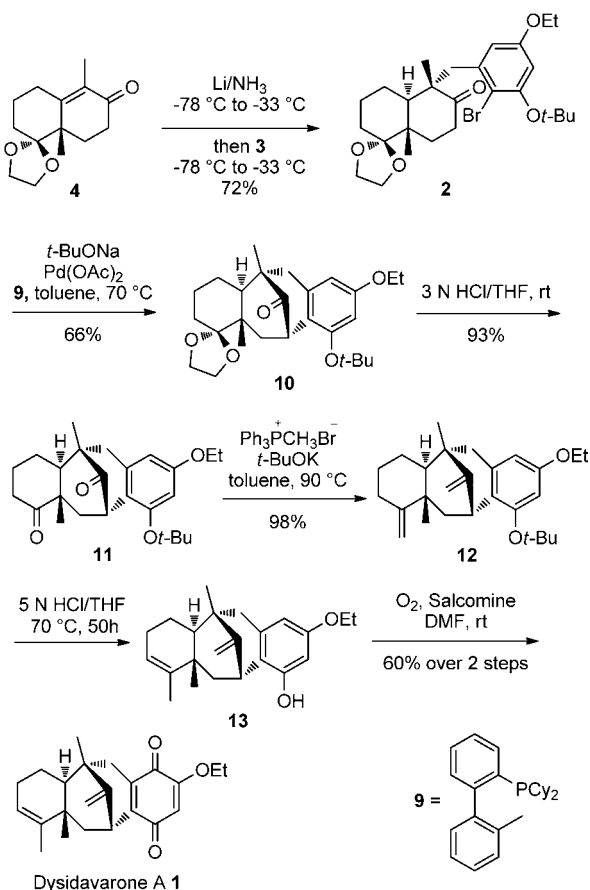
(11) Hagiwara, H.; Uda, H. *J. Org. Chem.* **1988**, *53*, 2308–2311.

(12) Bredereck, H.; Hennig, I.; Rau, W. *Chem. Ber.* **1953**, *86*, 1085–1095.

(13) Tatsuta, K.; Furuyama, A.; Yano, T.; Suzuki, Y.; Ogura, T.; Hosokawa, S. *Tetrahedron Lett.* **2008**, *49*, 4036–4039.

(14) Holcombe, J. L.; Livinghouse, T. *J. Org. Chem.* **1986**, *51*, 111–113.

Scheme 3. Completion of the Total Synthesis of Dysidavarone A



required significantly longer reaction times. Notably, this advanced application²² of the method in complex target synthesis proceeds in an unusual 6-*endo* mode.

After successful formation of the bridged eight-membered ring, ketal **10** was deprotected with 3N hydrochloric acid.^{16d} Afterward, both carbonyl-functions of compound **11** were methenylated by $\text{Ph}_3\text{P}^+\text{CH}_3\text{Br}^-$ and *t*BuOK.²³

Subsequent attempts to rearrange the terminal double bond **12** to **13** with RhCl_3 ^{16d} or iodine²⁴ failed, resulting in the cleavage of the *tert*-butoxy group and formation of a variety of byproducts. Deprotection was also evaluated with TFA in DCM²⁵ and TFMS in trifluoroethanol,¹⁴ but both reagents likewise resulted in various side products.

(21) (a) Biscoe, M. R.; Buchwald, S. L. *Org. Lett.* **2009**, *11*, 1773–1775. (b) Hellal, M.; Singh, S.; Cuny, G. D. *J. Org. Chem.* **2012**, *77*, 4123–4130.

(22) (a) MacKay, J. A.; Bishop, R. L.; Rawal, V. H. *Org. Lett.* **2005**, *7*, 3421–3424. (b) Liao, X.; Stanley, L. M.; Hartwig, J. F. *J. Am. Chem. Soc.* **2011**, *133*, 2088–2091. (c) Bhat, V.; Allan, K. M.; Rawal, V. H. *J. Am. Chem. Soc.* **2011**, *133*, 5798–5801. (d) Solé, D.; Vallverdú, L.; Solans, X.; Font-Bardia, M.; Bonjoch, J. *J. Am. Chem. Soc.* **2003**, *125*, 1587–1594. (e) Solé, D.; Peidró, E.; Bonjoch, J. *Org. Lett.* **2000**, *2*, 2225–2228.

(23) Fitjer, L.; Quabeck, U. *Synth. Commun.* **1985**, *15*, 855–864.

(24) Ling, T.; Xiang, A. X.; Theodorakis, E. A. *Angew. Chem., Int. Ed.* **1999**, *38*, 3089–3091.

(25) Tae, H. S.; Hines, J.; Schneekloth, A. R.; Crews, C. M. *Org. Lett.* **2010**, *12*, 4308–4311.

(26) Eder, U.; Haffer, G.; Neef, G.; Sauer, G.; Seeger, A.; Wiechert, R. *Chem. Ber.* **1977**, *110*, 3161–3167.

Table 1. Results of the α -Arylation of **2**

entry	catalyst ^a /ligand	base	solvent	temp	yield
1	$\text{PdCl}_2(\text{PPh}_3)_2/-$	Cs_2CO_3 ^b	THF	75–100 °C	
2	$(\text{DtBPF})\text{PdCl}_2/-$	<i>t</i> -BuONa ^c	THF	rt–75 °C	
3	$(\text{DtBPF})\text{PdCl}_2/-$	<i>t</i> -BuONa ^d	THF	80 °C	
4	$\text{Pd}(\text{OAc})_2/-$	<i>t</i> -BuONa ^d	toluene	80 °C	
5	$\text{Pd}(\text{OAc})_2/\text{P}(t\text{Bu})_3$	<i>t</i> -BuONa ^d	toluene	80 °C	
6	$\text{Pd}(\text{OAc})_2/\mathbf{9}$	<i>t</i> -BuONa ^d	toluene	70 °C	66%
7	XPhos-Precat/ [–]	<i>t</i> -BuONa ^d	toluene	80 °C	43%

^a Catalyst loading: 10 mol %, except for entry 2, where 2 mol % catalyst were used. ^b 3 equiv base was used. ^c 1.1 equiv base. ^d 1.3 equiv base was used.

Finally, we discovered that 5N HCl in THF²⁶ not only achieved deprotection, but also resulted in the required rearrangement of the *exocyclic* double bond to the more stable *endocyclic* olefin after prolonged reaction times. The free phenol **13** proved fairly stable in solution but decomposition was observed upon concentration. Therefore, it was used directly for the final oxidation with Salcomine [*N,N'*-bis(salicylidene)ethylene-diamino-cobalt(II)] under an O₂-atmosphere^{16d} to yield dysidavarone A with a yield of 60% over both steps (Scheme 3). The identity of the synthesized material with natural dysidavarone A was confirmed by NMR-, mass-, and CD-spectral data,^{1,27} which also proves the full stereostructure of this class of compounds in general.

With synthetic dysidavarone A in hand the biological potency of this scarce natural product could be studied in more detail. As shown in Table 2, it was evaluated against various microorganisms and cell lines demonstrating potent inhibitory effects against Gram-positive bacteria (Table 2, entries 8–15), in particular against various *Staphylococci* with activities in low or even below $\mu\text{g/mL}$ concentrations (Table 2, entries 11–15). Furthermore, it showed promising antiproliferative potencies against cancer cell lines (Table 2, entries 17, 18), while no inhibitory activity against various fungi/yeast (Table 2, entries 1–3) and Gram-negative bacteria (Table 2, entries 4–7) was observed. Likewise, dysidavarone A showed no anti-inflammatory activities (see Supporting Information section).

To attain further hints about the mode of action, dysidavarone A treated cells were screened on several apoptosis markers using U-2 OS cells. The cultured cells were stained by labeling mitochondria, endoplasmic reticulum, lysosomes, and nuclei and inspected by fluorescence microscopy (see Supporting Information section). As shown in Figure 1, treated cells showed striking alterations compared to the control population. In the course of treatment a

(27) Synthetic dysidavarone A was a crystalline compound (mp 98–103) and had an optical rotation of +125, while natural dysidavarone A was reported as an oil with an optical rotation of +30. This discrepancy may possibly be caused by a higher purity of the synthetic material as compared to the natural material, as evidenced from the NMR spectra supplied in the isolation paper.

Table 2. MIC₅₀ and GI₅₀ Values of Dysidavarone A **1**

entry	test organism	MIC ₅₀ [μg/mL]
1	<i>Mucor hiemalis</i>	~64
2	<i>Pichia anomala</i>	~64
3	<i>Candida albicans</i>	>64
4	<i>Escherichia coli</i> TolC	~64
5	<i>Escherichia coli</i> DH5α	>64
6	<i>Chromobacterium violaceum</i>	>64
7	<i>Pseudomonas aeruginosa</i> PA14	>64
8	<i>Bacillus subtilis</i>	>64
9	<i>Enterococcus faecalis</i> DSM20478	>64
10	<i>Enterococcus faecium</i> DSM20477	~64
11	<i>Micrococcus luteus</i>	5.5 ± 0.2
12	<i>Staphylococcus aureus</i> DSM346	7.1 ± 2.1
13	<i>Staphylococcus aureus</i> DSM11822 (multidrug resistant)	9.9 ± 0.8
14	<i>Staphylococcus aureus</i> N315 (methicillin resistant)	4.0 ± 0.1
15	<i>Staphylococcus aureus</i> Newman	6.5 ± 0.6
16	<i>Staphylococcus carnosus</i> DSM20501	0.2 ± 0.1
		GI ₅₀ [μg/mL]
17	human HL-60 myeloid leukemia cell line (ACC-3)	1.65
18	human HepG2 hepatocellular carcinoma cell line (ACC-180)	4.26

significant disruption of lysosomal integrity (deacidification) was observed. In addition, unusual pore formation took place which was accompanied by specific morphological alterations of the cells, that is, membrane blebbing and chromatin condensation. The macroscopic effects of **1** partially resemble those of bacterial pore-forming toxins²⁸ and may suggest that these compounds trigger a lysosomal dysfunction that culminates in the release of cathepsins from lysosomes in the cytosol, which in turn causes proteolytic cell damage and may activate the mitochondrial apoptosis pathway.²⁹

In summary, the first total synthesis of dysidavarone A was achieved in a highly concise route in 10 steps (longest linear sequence) with a total yield of 11% and confirms the

(28) Kennedy, C. L.; Smith, D. J.; Lyras, D.; Chakravorty, A.; Rood, J. I. *PLoS Pathogens* **2009**, *5*, e1000516.

(29) Cesena, M. H.; Pegana, K.; Spesa, A.; Turka, B. *Exp. Cell. Res.* **2012**, *313*, 1245–1251.

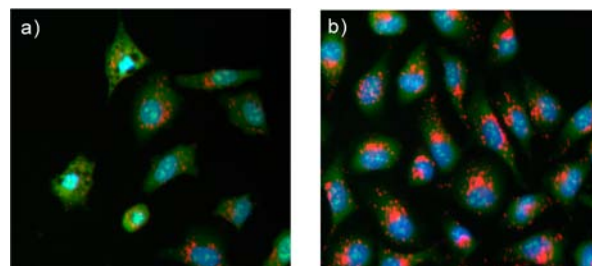


Figure 1. Changes of cellular morphology and lysosomal pH of cultivated U-2 OS cells upon 3 h treatment with 20 μg/mL dysidavarone A (a) in comparison to control cells (b). Cells were incubated and stained with acridine orange (red: acidic lysosomes; green: neutral compartments) and Hoechst 33342 (blue: nuclei).

unique 3D structure of this class of quinone sesquiterpenes. Key transformations of the convergent synthesis include a stereoselective reductive alkylation of a Wieland-Miescher type ketone and an advantageous α-arylation of a highly hindered elaborate ketone using the Buchwald ligand. The concise route enabled access to sufficient material for further biological evaluation of this scarce metabolite, revealing potent antibacterial and antiproliferative activities by specifically changing the morphology of treated cells. Present studies are now directed to further analyze and potentially use this promising biological potency.

Acknowledgment. This work was generously supported by the D.F.G. (SFB 623). The authors thank Sebastian Essig, Michael Dieckmann, Thomas Debnar (University of Heidelberg), Dr. Manuel Kretschmer (Columbia University New York) and Dr. Aubry Miller (German Cancer Research Center, Heidelberg) for helpful suggestions in devising the synthetic route as well as Andreas J. Schneider (University of Bonn) for HPLC-support and Friederike Eberhagen (University of Bonn) for technical support.

Supporting Information Available. Experimental procedures, spectral data and copies of ¹H- and ¹³C NMR spectra for all new compounds and details of biological experiments. This material is available free of charge via the Internet at <http://pubs.acs.org>.

The authors declare no competing financial interest.